ENHANCEMENT OF CONVECTIVE HEAT TRANSFER USING MAGNETICALLY FLAPPING FIN ARRAY

T.-B. Nguyen[1], D. Liu[1], H. Raut[2], A. Bhattacharya[2,3], A. Sharma[2], T. Tran[1*]

[1]School of Mechanical and Aerospace Engineering, Nanyang Technological University, Singapore
[2]Department of Mechanical Engineering, Indian Institute of Technology Bombay, India
[3]Department of Applied Mechanics, Indian Institute of Technology Delhi, Hauz Khas, India

ABSTRACT

Electronic devices with high power density require efficient and compact heat transfer management methods. While passive fins have been routinely used for heat dissipation, they usually have a limited range of operating conditions in electronic applications. In this study, we explore experimentally and numerically active enhancement of convective heat transfer using a magnetically actuated array of fins. In our experiments, the fins are rectangular nickel strips attached to a silicon substrate via flexible joints and actuated by an alternating electromagnetic field. We observe that angular oscillation of the fins leads to significant enhancement in heat transfer coefficient. Specifically, at high actuation frequencies and amplitudes, the heat flux enhancement for a fixed wall temperature may be up to 100%. We examine the scaling between the measured heat flux, frequency, and temperature difference. For an actively cooled substrate, the Nusselt number is primarily determined by forced convection due to fin motion, while the contribution from buoyancy is weak. In our two-dimensional numerical simulations, we use a dual-grid immersed boundary method for a flow geometry consisting of a single actuated fin in a rectangular domain. The simulated flow field and isotherms indicate the formation of thin thermal boundary layers on the fin and base plate. The tip vortices shed by the fin are instrumental in mixing and transport of temperature field. The active cooling principle described in this work may be employed as an efficient and compact thermal management method for small electronic devices with high power densities.

1. INTRODUCTION

Two-phase heat transfer processes have high heat transfer rate with the drawback of bulky heat sink device. Therefore, single-phase liquid cooling appears to be the most suitable approach for applications requiring moderate heat transfer rates over a compact area [1-2]. In this work, we demonstrate enhancement of convective heat transfer using electro-magnetic actuation of an array of nickel strips. We first experimentally investigate the dependence of the net heat flux through the substrate on the substrate temperature and the frequency of actuation. Our measurements indicate that it is possible to control the heat transfer enhancement by adjusting the frequency of actuation. Our data analysis also suggests that the actuation-induced increase in characteristic velocity of the fluid leads to a reduction in the thermal boundary layer thickness, and subsequently causes the enhancement in net heat flux. We next use numerical simulations based on sharp-interface immersed boundary method to simulate flow and heat transport around a single actuated fin at different frequencies. The simulations indicate the presence of robust thermal boundary layers on both fin and base plate, as well as tip vortices at the fin. The attached and detached tip vortices can interact with each other, and lead to transport of hot fluid parcels away from the fin. Both the experiments and numerical simulations indicate that the average Nusselt number scales as the square root of the Reynolds number based on fin actuation frequency.

2. METHODOLOGY

In our experimental setup (Fig. 1a), the working liquid (FC-72) is kept inside a glass cuvette of dimension 10×10×45 mm. The substrate is made of a 500 μm thick silicon layer glued to a copper rod using thermal silicon paste. The copper rod is heated and controlled by cartridge heater via a PID controller. Three Pt100 thermal sensors (T_1, T_2, and T_3, Fig. 1a) are inserted at evenly spaced positions

*Corresponding Author: ttran@ntu.edu.sg (Tuan Tran)

along the axis of the copper rod to measure the net heat flux q and the surface temperature T. The temperatures T_1 to T_6 (Fig. 1a) are measured and recorded by a digital datalogger. The average liquid temperature T_l is obtained by taking the average value of T_4, T_5 and T_6. It is also worth noting that temperature measurements are only taken at the steady state. The steady-state temperatures are then used to calculate the heat flux q and the temperature difference $\Delta T = T - T_l$. The array of nickel fins is fabricated on silicon substrate and is actuated by an oscillating magnetic field generated by a pair of electromagnets positioned on two sides of the boiling chamber, as shown in Fig. 1a. The oscillating magnetic field are driven by a sine wave voltage signal U_d (Fig. 1c). The fins' actuation frequency f, is varied from 5 Hz to 35 Hz. In Fig. 1b, we show several representative snapshots of the actuated fins during an oscillating cycle. Each experiment starts by heating the substrate gradually to reach a target surface temperature T. Once the system reaches the steady state, the electromagnet is switched on to actuate the fins with frequency f. We then calculate the corresponding heat flux q and measure the liquid temperature T_l. The experimental uncertainty is obtained by repeating the experiment five times for each experimental condition.

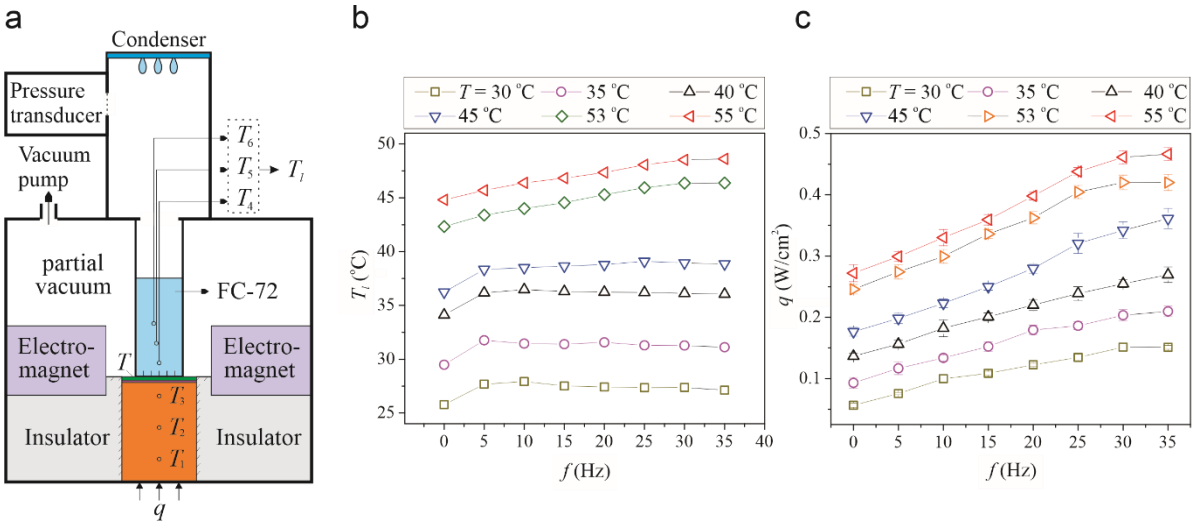

Figure 1: (a) Schematic (not to scale) of the experimental setup. (b) Dependence of the average liquid temperature T_l on actuation frequency f for different wall temperatures T. (c) Dependence of heat flux q on actuation frequency f for different wall temperatures T. Error bars indicate the standard deviation of the heat flux readings.

3. RESULTS AND DISCUSSIONS

3.1 Results from experiments

We now examine the effect of flow actuation using flapping fins by measuring the dependence of heat flux q on the actuation frequency f for different values of the wall temperature T (Fig. 1c). The upper limit of the temperature range (set at 55 ℃) is slightly lower than boiling point of the working liquid ($T_b = 56$ ℃ for FC-72). For a fixed T, we find that q increases monotonically with f, indicating that flow actuation caused by flapping fins significantly enhances the overall heat flux from the substrate. For each surface temperature T, the enhancement of heat flux, q, due to actuated frequency, f, can be estimated as $\%q_E = (q_{35\text{Hz}} - q_{0\text{Hz}})/q_{0\text{Hz}} \times 100\%$, where $q_{0\text{Hz}}$ and $q_{35\text{Hz}}$ are heat flux values measured with fins arrays actuated at f = 0 Hz and 35 Hz respectively. The maximum enhancement of heat flux, $\%q_E = 100\%$, can be achieved at surface temperature T = 30 ℃. The heat flux enhancement gradually reduces to $\%q_E = 60\%$ when surface temperature T reaches 55 ℃, close to the boiling point.

In Fig. 1b, we plot the average liquid temperature T_l versus the frequency f for different values of T. We note that, for a fixed wall temperature, there is a significant jump in T_l when f is increased from zero to f = 5 Hz. Subsequently, T_l increases gradually with actuation frequency and approaches a plateau

for f > 5 Hz. The jump in T_l at f = 5 Hz originates from the flapping fins, which enhance mixing of the bulk fluid and thus leads to larger temperature differences between the bulk fluid and the heated surface across the thermal boundary layer. Furthermore, T_l (and therefore $\Delta T = T - T_l$) stays approximately constant with increasing f. By balancing the heat flux going through the surface due to convection $q = h\Delta T$ with heat conduction at the liquid near the surface $q = -kdT/dx\,|x = x_w$, we can obtain the convective heat transfer coefficient $h = -k/\Delta T \times dT/dx \mid x = x_w$. Here k is the thermal conductivity of the liquid, and $dT/dx \mid x = x_w$ is the temperature gradient at the heated surface ($x = x_w$). For fluids with large Prandtl number, $dT/dx \mid x = x_w \approx -\Delta T/\delta_T$, where δ_T is the effective thermal boundary layer thickness. Therefore, if temperature difference ΔT is constant with respect to f, and thermal conductivity of the liquid does not vary with temperature, the monotonic increase of q (or h) with f (Fig. 1c), suggests that the enhancement in heat flux is caused primarily by a reduction in the effective thickness of the thermal boundary layer δ_T at the surface as a result of flapping fins.

To further understand the dependence of the heat flux q on the actuation frequency f and the wall temperature T, or equivalently the temperature difference $\Delta T = T - T_l$, we examine the non-dimensional relationship Nu = $\mathcal{F}$(Re, Gr, Pr), where Nu = $qL/(\Delta T k)$ is the Nusselt number (non-dimensional heat flux), Gr = $g\beta\Delta T L^3/\nu^2$ the Grashoff number (nondimensional buoyancy), Pr = $\nu\rho Cp/k_l$ the Prandtl number, and Re = $f\,L^2/\nu$ the Reynolds number (non-dimensional inertia). Here L = 1.5 mm denotes the height of the fin, g is the gravitational acceleration, k is the thermal conductivity of the liquid, ν the kinematic viscosity, β the coefficient of expansion, C_p the specific heat capacity, and ρ the density. Since Pr is constant in our experiments, we focus on the effect of Gr and Re on Nu.

In the absence of any actuation, i.e., f = Re = 0, the Nusselt number scales as Nu ~ $Gr^{0.63}$ (Fig. 2a). This scaling is consistent with past measurements [3], where a correlation of the form Nu ~ $Ra^{0.57}$ was observed for natural convection over fins. Here, similar to the Grashoff number Gr, the Rayleigh number Ra is also proportional to ΔT. This scaling, however, departs significantly from the Nu ~ $Gr^{1/4}$ scaling that one expects if a thermal boundary layer based on buoyant wall plumes are responsible for the heat transfer [4, 5].

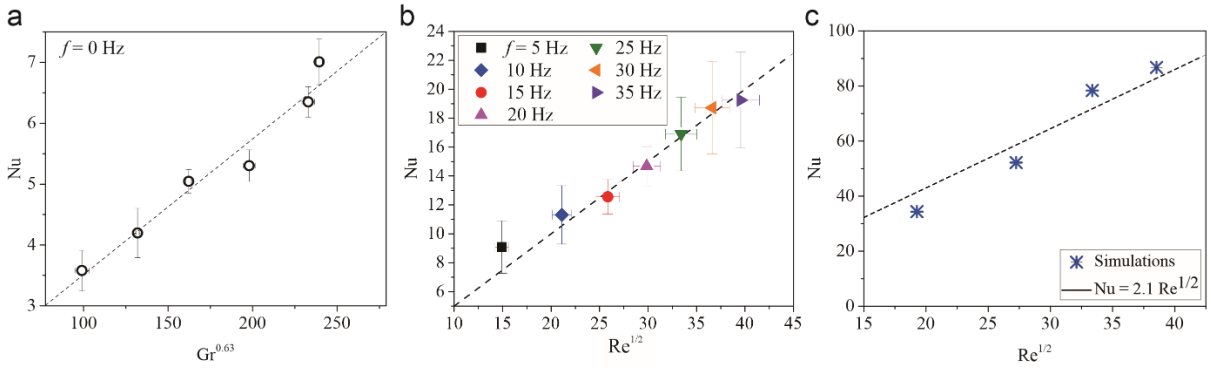

Figure 2: (a) Relation between Nu and $Gr^{0.63}$ for the passive case (f = 0). The dashed line indicates the scaling Nu ~ $Gr^{0.63}$. (b) Relation between Nu and $Re^{1/2}$ for different actuation frequencies f.

At high actuation frequency f, we expect Nu to be determined mostly by Re. In such a situation, the convective velocity of the fluid is proportional to the actuation frequency and fin height, $U \sim f\,L$. For FC-72, Pr≫1, indicating that in the presence of forced convection, the thickness δ_T of the thermal boundary layer is less than the thickness δ of the velocity boundary layer at the wall. In such cases, it can be readily shown that $\delta_T/L \propto \mathrm{Re}^{-1/2}\mathrm{Pr}^{-1/3}$ [5]. The net heat flux is then given as $q \sim k(T - T_l)/\delta_T = k((T - T_l)/L)\mathrm{Re}^{1/2}\mathrm{Pr}^{1/3}$, indicating that Nu scales as $\mathrm{Nu} = qL/(k\Delta T) \sim \mathrm{Re}^{1/2}\mathrm{Pr}^{1/3}$. In Fig. 2b, we note that Nu indeed appears to vary approximately linearly with $Re^{1/2}$, although there is also significant scatter in the data at higher values of f. It was shown [6] using dimensional analysis and

conservation laws, i.e., mass, momentum, and energy conservation, that the Nusselt number should follow the scaling $\mathrm{Nu} \sim \mathrm{Re}^{1/2}\, g(\mathrm{Gr}^{1/4}\mathrm{Re}^{-1/2})$ for combined forced and natural convection, with g asymptotically tending to a constant for $\mathrm{Gr}^{1/4}\mathrm{Re}^{-1/2} \longrightarrow 0$. Interestingly, such a trend in $g(\mathrm{Gr}^{1/4}\mathrm{Re}^{-1/2})$ was also observed for forced convection on a heated vertically oriented plate undergoing periodic longitudinal oscillations [7], whereby Re was determined based on the frequency of the plate oscillation. We however do not see a significant dependence of Nu on Gr in our experiments with flapping fins. In [7], a similar weak dependence of Nu on Gr is observed for the range of $\mathrm{Gr}^{1/4}\mathrm{Re}^{-1/2}$ over which our experiments have been conducted ($0.1 < \mathrm{Gr}^{1/4}\mathrm{Re}^{-1/2} < 0.55$).

3.2 Results from numerical simulations

In this work, we have imposed a super-heat of $\Delta T = T_w - T_0 = 5$ K for all the numerical simulations. The thermophysical properties of FC-72 have been used for these simulations, so that liquid density is ρ = 1680 kg/m^3, specific heat capacity is C_p = 1100 J/(kgK), dynamic viscosity is μ = 0.00064 Pas, thermal conductivity is k_l = 0.057 W/(mK) and coefficient of thermal expansion is $\beta = 1.56\times10^{-3}$. These properties correspond to Grashoff number Gr = 1780, or $\mathrm{Gr}^{0.63}$ = 111, which falls well within the range of Gr covered in experiments (Fig. 2a). The Prandtl number is Pr = 12.35, which implies that the thermal boundary layer will be much thinner than the momentum boundary layer. The actuation frequency is varied over $f = \{0, 10, 20, 30, 40\}$ Hz, where f = 0 Hz corresponds to no actuation. Besides the time period $1/f$ and length of the fin L, we use the length scale l_0 = 1 mm and time scale $t_0 = 10^{-2}$ s to nondimensionalize the parameters in this section. The integral of the heat flux (per unit depth) from the fin $Q_{fin}(t)$ and the base plate $Q_{plate}(t)$ has been measured at every time instant t. The time series of corresponding Nusselt number can then be calculated as $\mathrm{Nu}_{plate}(t) = h_{plate}(t)L/k_l$ and $\mathrm{Nu}_{fin}(t)\ h_{fin}(t)L/k_l$, where $h_{fin} = Q_{fin}/(\Delta T L_x)$ and $h_{plate} = Q_{plate}/(\Delta T L_x)$ are heat transfer coefficients. The total Nusselt number is then defined as $\mathrm{Nu}(t) = \mathrm{Nu}_{\mathrm{fin}} + \mathrm{Nu}_{\mathrm{plate}}$. To test the grid convergence properties of the solver, we first conduct simulations at f = 20 Hz with grid resolutions $N_x \times N_y = 128 \times 192$ (low resolution), $N_x \times N_y = 160 \times 240$ (medium resolution) and $N_x \times N_y = 200 \times 300$ (high resolution). The details of this analysis are discussed in the supplementary material. Based on the optimized grid-convergence analysis, we use the medium-resolution grid ($N_x \times N_y = 160 \times 240$) for the rest of the simulations discussed below. Simulations with fin actuation have been evolved in time over at least 10 actuation cycles (i.e., for $tf > 10$). For the case with f = 0 we have to run the simulation for a much longer time (up to t/t_0 = 600) to achieve a steady state in Nusselt number.

Snapshots of temperature and velocity field from the simulation at f = 0 Hz (no actuation) show that a hot plume develops above the fin (Fig. 3a, snapshot I), and eventually departs, leaving behind a thick thermal boundary layer on both the fin and the base plate (Fig. 3a, snapshot II). The plume from the fin tip orients itself horizontally due to the asymmetric downdrafts and updrafts induced in the flow domain (Fig. 3a, snapshot III). The Nusselt number stays low (Nu≪1) until the plume departs, at around $t/t_0 \approx 350$, after which it plateaus to Nu ≈ 9.3 at large time.

We next discuss the characteristics of temperature and flow field with actuated fins ($f > 0$). Snapshots of temperature and velocity field at f = 20 Hz show the presence of a tip vortex at the upper end of the fin at almost all times (Fig. 3b). The tip vortex forms due to the pressure difference between the fore and aft sides of the fin and is shed as soon as the fin reverses direction. The tip vortex attached to the fin essentially mixes cold fluid above the fin with the warmer fluid below the fin (Fig. 3b, snapshot I). The interaction between the vortices shed by the fin plays an important role in mixing and transporting heat in the flow domain. Eventually, due to vigorous mixing of fluid by these vortices, very thin thermal boundary layers form at the base plate and the fin (Fig. 3b, snapshot III). The interaction between the attached tip vortex and previously detached vortex led to frequent formation of vortex pairs. Fig. 3c shows snapshots from the simulation at f = 40 Hz over a quarter oscillation cycle ($\dot{\theta} > 0$). Initially, we observe a detached counterclockwise (CCW) vortex to the left of the fin (Fig. 3c, snapshot I), and a clockwise (CW) tip vortex forming behind (to the right) of the fin. The left-ward motion of the fin

squeezes the detached CCW vortex upwards, while the CW tip vortex stays attached to the fin (Fig. 3c, snapshot II). Eventually, the CW tip vortex is shed, and then interacts with the CCW detached vortex. The velocities induced by the CW and CCW vortices on each other leads to formation of a vortex pair, and transport of heated fluid parcels engulfed by the vortices away from the fin. For all the simulations with $f > 0$, we find that Nu increases sharply after around 4 actuation cycles ($tf > 4$), and then fluctuates around an approximately constant value after 6 actuation cycles ($tf > 6$). The average Nusselt number (cycle-averaged over last 4 actuation cycles) appears to scale reasonably well with $\mathrm{Re}^{1/2}$, which is consistent with the experimental results (Fig. 2c). The Nusselt number for $f > 0$ is clearly much larger than $\mathrm{Nu} \approx 9.3$ obtained without any fin actuation. Also, typical time scale ($t/t_0 \approx 350$) for the first plume to depart for the case with zero actuation is much longer than the time period ($t/t_0 = 20$) for even the case with the slowest actuation of $f = 5$ Hz, which explains the low sensitivity of Nu with respect to Gr in the presence of fin actuation.

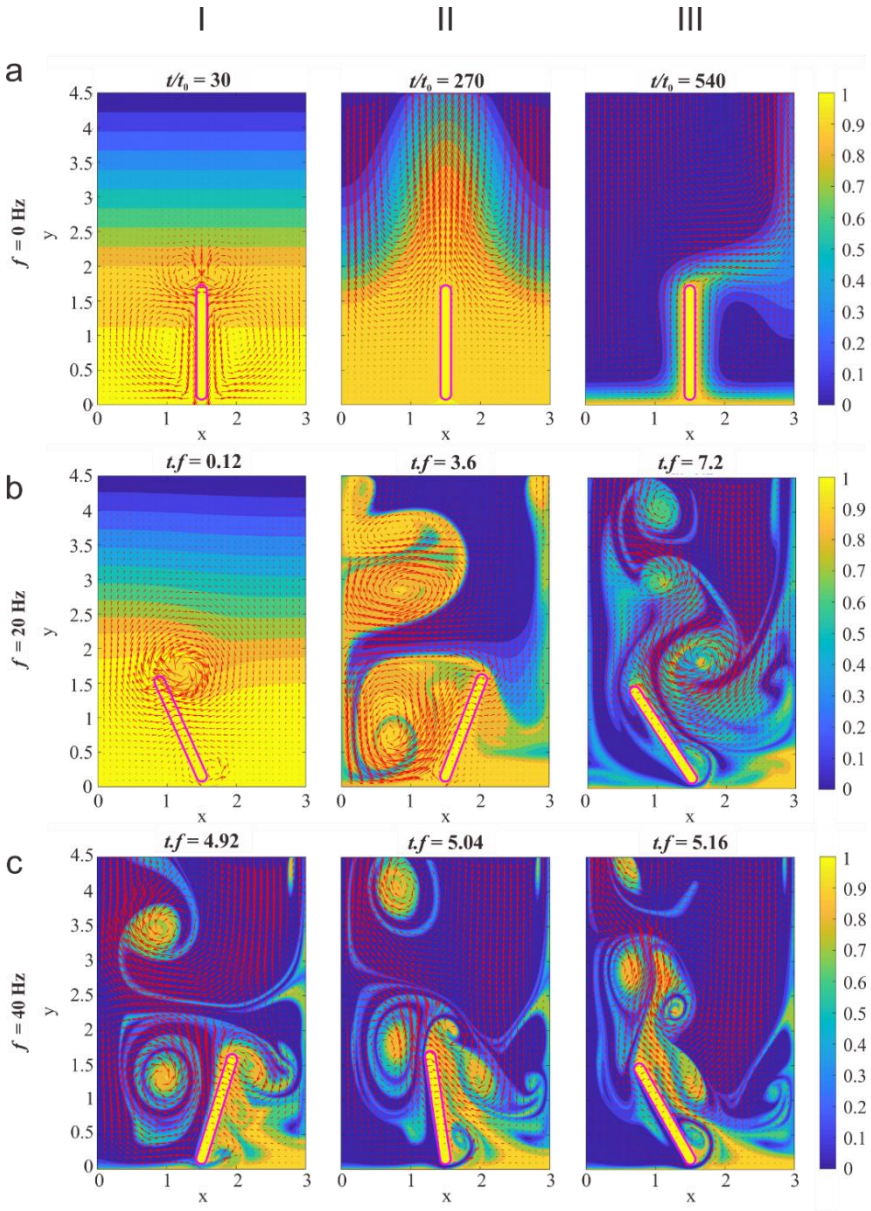

Figure 3: Snapshots showing temperature iso-contours and velocity vector field (red arrows) at different time instances: (a) $f = 0$ Hz (no fin actuation) over a long time, (b) $f = 20$ Hz over 7.2 actuation cycles (c) $f = 40$ Hz over 0.25 actuation cycle. Distance along the axes, x and y, has been non-dimensionalized with respect to length scale l0. Non-dimensional time t/t_0 for each snapshot has been indicated above the figure.

The most notable discrepancy here appears to be the over-prediction of Nu (by a factor of 4) of the experimental values by the simulations (Fig. 2b vs Fig. 2c). One of the main reasons for this quantitative discrepancy is that, while flow domain in the numerical simulation has a width $L_x = 2L$, an adiabatic boundary condition ($\partial T/\partial n = 0$) is used for temperature at the lateral boundaries. On the other hand, the fins are surrounded by neighbouring fins at $T = T_w$ in the experiments, which can lead to significantly thicker boundary layers (i.e., lower Nusselt number) at fin and plate surface for a given superheat ΔT. The other obvious source of error in the numerical simulations is that we solve for the flow field in two-dimensions, and therefore the three-dimensional effects near the ends of the fins will not be captured in the simulations. The no-penetration condition on the lateral boundaries, as opposed to a periodic arrangement of fins in the experiments, may also lead to significant quantitative differences in Nusselt number predicted by the simulations and experiments.

4. CONCLUSIONS

In summary, we have experimentally demonstrated a novel and robust method for enhancing heat transfer on a substrate using electromagnetic-induced actuation of nickel fins. We achieved localized heat transfer enhancement up to 100% using single-phase liquid cooling. For any given wall temperature *T*, the bulk temperature does not change significantly with actuation frequency, indicating that any enhancement in heat flux results from a systematic reduction of the thermal boundary layer thickness in the presence of actuation. In general, it appears that for active fins, the thermal boundary layer thickness is governed by the convective fluid velocity induced by the flapping fins. The snapshots of flow field confirm the presence of thin thermal boundary layers at the surface of base plate and fin. The simulations also highlight the importance of tip vortices shed by the fin towards transporting and mixing of thermal energy. The slow growth and departure of plumes for the case with zero actuation is also consistent with the insensitivity of experimental results with respect to Grashoff number. The results from this work show that increasing the characteristic velocity scale of the fluid flow using electromagnetically actuated structures can be used to significantly enhance the rate of heat transfer from heated substrates.

ACKNOWLEDGEMENTS

This work was supported by the Nanyang Technological University (NTU), Ministry of Education (MOE, grant number MOE2018-T2-2-113), Singapore, and Department of Science and Technology (DST), India. T.B. Nguyen acknowledges the support from MOE. A.B. acknowledges project staff and travel support from (DST) (No: INT/SIN/P-02).

REFERENCES

[1] A. M. Hussein, R. A. Bakar, K. Kadirgama, Study of forced convection nanofluid heat transfer in the automotive cooling system, *Case Stud. Therm. Eng.* **2** (2014) 50–61

[2] D. A. Staton, A. Cavagnino, Convection heat transfer and flow calculations suitable for electric machines thermal models, *IEEE Trans. Ind. Electron.* **55** (10) (2008) 3509–3516

[3] S. A. Nada, Natural convection heat transfer in horizontal and vertical closed narrow enclosures with heated rectangular finned base plate. *Int. J. Heat Mass Transf.* **50** (3-4) (2007) 667–679

[4] A. B. Cohen, M. Iyengar, A. D. Kraus, Design of optimum plate-fin natural convective heat sinks. J. Electron. Packag. **125** (2) (2003) 208–216

[5] A. Bejan, Turbulent Boundary Layer Flow. In: *Convection Heat Transfer*, John Wiley Sons, Ltd, (2013), pp. 320–368

[6] A. Acrivos, Combined laminar free-and forced-convection heat transfer in external flows. *AIChE Journal* **4** (3) (1958) 285–289

[7] K. K. Prasad, V. Ramanathan, Heat transfer by free convection from a longitudinally vibrating vertical plate. *Int. J. Heat Mass Transf.* **15** (6) (1972) 1213–1223